BBAA VI International Colloquium on:
Bluff Bodies Aerodynamics & Applications
Milano, Italy, July, 20-24 2008

FLOW FLUCTUATIONS AND VORTICITY DYNAMICS IN THE NEAR WAKE OF A TRIANGULAR PRISM IN CROSS-FLOW

Guido Buresti and Giacomo Valerio Iungo

Dipartimento di Ingegneria Aerospaziale
Università di Pisa, Via G. Caruso 8, 56122 Pisa, Italy
e-mail: g.buresti@ing.unipi.it, giacomo.iungo@ing.unipi.it

Keywords: Bluff body aerodynamics, prisms, wakes, flow fluctuations, vorticity dynamics.

Abstract. *The results are described of experiments carried out to investigate on the connection between the flow fluctuations and the dynamics of different vorticity structures in the wake of a prism with equilateral triangular cross-section, aspect-ratio h/w = 3 (where h and w are the prism height and width, respectively), and placed vertically on a plane with its apex edge against the incoming flow. Flow visualizations, hot-wire velocity surveys and pressure measurements are analysed for the model in the original configuration and with geometrical modifications along its edges, conceived in order to interfere with the evolution of the various vorticity structures. In the wake of the original model, fluctuations at three prevailing frequencies are present, with different relative intensities depending on the wake region. In particular, the frequency connected with alternate vortex shedding from the lateral vertical edges of the prism, with a Strouhal number St = fw/U ≅ 0.16 (HF), dominates in the zones outside the lateral boundary of the wake, for vertical positions below z/h = 0.9. A lower frequency, at St ≅ 0.05 (LF), is found to prevail in the velocity fluctuations in the whole upper wake, for downstream distances x/w ≥ 1.5; this frequency is associated with a vertical, in-phase, oscillation of the vorticity structures detaching from the free-end. Fluctuations are also observed at an intermediate frequency St ≅ 0.09 (IF), and prevail in positions corresponding to the downstream boundary of the recirculation region in the central part of the near wake. Measurements of the mean and fluctuating pressures over the upper and rear surfaces of the model confirm the suggestion that the origin of the IF may be an oscillation of the transversal vorticity sheet bounding the recirculation region behind the body. Geometrical modifications to the lateral edges of the model, introduced to alter the vortex shedding, produce a lowering of the HF, directly related to the increase of the mean wake width, and the IF is found to follow a similar decreasing trend. Conversely, small plates inserted along the front edges of the model free-end do not alter the frequency, energy and regularity of the LF fluctuations in the upper part of the wake; this result probably derives from the fact that, in spite of the highly irregular free-end edge, the mechanism of roll-up of the vorticity shed from the sides of the plates is still strong enough to generate the axial vortices, even if with a different formation process. The forces acting on the various models are also measured.*

1 INTRODUCTION

The prediction of the unsteady aerodynamic loads on three-dimensional bluff bodies is of interest for many engineering applications, as, for instance, the design of buildings under the action of the wind. These unsteady loads are produced by velocity fluctuations connected with the dynamics of the vorticity structures present in the wake. Therefore, in order to achieve a satisfactory predictive capability of the aerodynamic loads on these types of bodies, the present understanding of wake flows must be increased through an accurate analysis of the velocity fluctuations and of their connection with the dynamic behaviour of the vorticity structures.

In particular, considering finite cylinders and prisms in cross-wind, the wakes are dominated by the velocity fluctuations induced by the alternate vortex shedding from the body sides, but further fluctuations at different frequencies may appear in the near wake, which are connected with the dynamics of the vorticity structures originated by the flow passing over the body free-end; these structures are considerably influenced by the shape of the body cross-section and by the wind orientation. In previous investigations ([1], [2], [3]), the fluctuating wake flow field of a prism with equilateral triangular cross-section, aspect-ratio $h/w = 3$ (where h is the prism height and w the width of its cross-section base), and placed vertically on a plane with its apex edge against the incoming flow, was characterized through hot-wire measurements. For this body shape and this direction of the flow, two strong counter-rotating vortices were found to detach from the free-end, and to significantly influence all the upper-wake flow field. Furthermore, fluctuations at three prevailing frequencies were singled out, with different relative intensities depending on the wake regions.

In particular, the frequency connected to alternate vortex shedding from the lateral vertical edges of the prism, corresponding to a Strouhal number $St = fw/U \cong 0.16$, was found to dominate for vertical positions below $z/h = 0.9$, and to be particularly strong in the regions just outside the lateral boundary of the wake. A lower frequency, at $St \cong 0.05$, was found to prevail in the velocity fluctuations on the whole upper part of the wake, and in particular above $z/h = 1.0$ for downstream distances $x/w \geq 1.5$. The interest of this frequency derives also from the fact that in [4] velocity fluctuations with a dominating frequency at 1/3 of the usual vortex shedding frequency had been found in the upper portions of the wake of a finite circular cylinder with a much higher aspect-ratio ($h/d = 25$), and had been shown to be capable of producing significant cross-flow oscillations when their frequency coincided with the natural one of the cylinder. A low-frequency peak in the velocity spectra was also detected in [5] aside the upper wake of finite circular cylinders, and in both these works it was suggested that this frequency might be related to oscillations of the tip vortices. In effect, by using time-frequency techniques for component extraction and cross-correlation analysis (described in detail in [6]), it was shown in [1] that the upper wake low frequency may be associated with a vertical, in-phase, oscillation of the vorticity structures detaching from the free-end.

A LES simulation of the same flow configuration, described in [7], provided values of the rms wake fluctuations that were in good agreement with those obtained from the hot-wire measurements reported in [2], in spite of being carried out at a lower Reynolds number ($Re = Uw/\nu = 10^4$ instead of $Re = 1.5 \cdot 10^5$). In particular, it confirmed the connection between the low frequency fluctuations and the oscillation of the counter-rotating axial vortices detaching from the body tip and of the sheets of vorticity wrapped around them. Furthermore, it allowed the shape of the upper boundary of the near wake to be characterized, and showed that the vorticity sheets shed from all the edges of the prism interact in a non-trivial way to give rise to a complex topology, with a striking difference between the vertical positions of the middle and lateral portions of the upper wake boundary. The role of the cross-flow vorticity component shed from the rear edge of the body free-end could also be highlighted.

In [3], wake velocity fluctuations at an intermediate frequency $St \cong 0.09$ were also observed, and were found to prevail in the symmetry plane $y/w = 0$, in positions corresponding to different downstream distances depending on the value of z/h. By using as a reference the numerical information provided by the abovementioned LES simulation, it was suggested that they may be caused by a flag-like oscillation of the sheet of transversal vorticity shed from the rear edge of the body free-end, and approximately lying along the downstream boundary of the recirculation region in the central part of the near wake.

In the present paper the results are described of experiments carried out to further investigate on the connection between the wake flow fluctuations and the dynamics of the different vorticity structures. Flow visualizations, hot-wire velocity surveys and pressure measurements are analysed for the model in the original configuration and with geometrical modifications along its edges, conceived in order to interfere with the evolution of the various vorticity structures, and thus to ascertain if connections exist between the various frequencies present in the wake. The forces acting on the various models are also measured.

2 EXPERIMENTAL SET-UP AND PROCEDURES

The tests were carried out in the subsonic wind tunnel of the Department of Aerospace Engineering of the University of Pisa, and the experimental set-up is sketched in Fig. (1), where the used reference frame is also shown. The model has an equilateral triangular cross-section, an aspect ratio $h/w = 3$ (with a base width $w = 90$ mm), and is positioned vertically on a plane, where the boundary layer thickness is approximately 10 mm, and may thus confidently be assumed not to affect the flow in the upper-wake region. The wind-tunnel turbulence level is about 0.9%, and most of the tests were carried out at a Reynolds number $Re = Uw/\nu = 1.5 \cdot 10^5$.

The model was connected to a support, positioned below the plane and inside a fairing, which was replaced by a six-component strain-gage balance when forces were measured. The flow visualizations were performed by injecting smoke upstream of the model with a probe, so that the shear layers detaching from the model edges could be highlighted; the light sheet was produced by a Magnum 1.1 Stocker Yale laser with a wavelength of $\cong 900$ nm and an output power of 750 mW. The pressure measurements were carried out using two Pressure Systems ESP-16HD electronic pressure scanners, each with 16 ports and transducers, which were previously calibrated. The pressure taps on the surfaces, about 0.5 mm in diameter, were connected to the respective ports through $\cong 400$ mm long plastic tubes, assuring that the highest frequency of interest (viz. that of vortex shedding) could be adequately described. From each port, signals comprising 2^{16} samples were acquired with a sampling rate of 2 kHz.

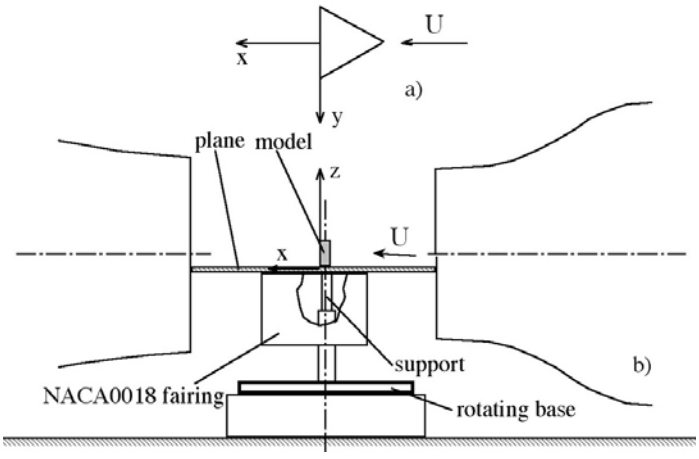

Figure 1: Experimental set-up. a) model orientation; b) test lay-out.

As for the velocity measurements, single-component Dantec type 55 hot-wire probes and an IFA AN 1003 A.A. Lab System anemometry module were used. After extensive preliminary tests, a sampling frequency of 2 kHz and a time-length of approximately 33 s were chosen for the acquisitions. The probes were used with their wire oriented horizontally, and were moved in the axial, vertical and transversal directions using a computer-controlled traversing support rig, which allowed detailed characterizations of the wake flow field to be obtained.

All the various dominating spectral components in the wake fluctuations are generally highly intermittent and with significant modulations, both in amplitude and frequency. The analysis of the velocity and pressure signals was then first carried out by using wavelet spectra, which are analogous but smoother than Fourier spectra for highly unsteady signals. Subsequently, a procedure based on the wavelet and Hilbert transforms, described in detail in [6], was used to extract and characterize the various dominating frequencies present in the signals. In brief, the energy wavelet maps, produced using a complex Morlet wavelet with a high value of the wavelet central frequency (to increase the frequency resolution and reduce the interference effects between adjacent components), are filtered by neglecting the wavelet coefficients outside a band centred at the frequency of interest. The inverse wavelet transform is then applied to obtain the time-series corresponding to the extracted component, which is a narrow-band signal whose modulations in amplitude and frequency may be characterized through a demodulation technique based on the construction, by means of the Hilbert transform, of its associated *analytic signal*. The time-variation of the amplitude and of the instantaneous frequency of the extracted component may thus be obtained and analysed. The instantaneous phase difference between two analogous components extracted from simultaneously acquired signals may also be obtained from their associated *cross-analytic signal* and from the *Hilbert Local Correlation Coefficient, HLCC,* which varies from −1 to +1 and gives the time variation of the contribution to the correlation between the two signals (see [6]).

3 RESULTS FOR THE ORIGINAL PRISM

3.1 Hot-wire measurements

The velocity signals acquired aside the wake of the original prism are characterized by the presence of a spectral peak around $St \cong 0.16$, which, through the analysis of the correlation between signals simultaneously acquired on the two sides of the wake, was shown to correspond to an alternate vortex shedding from the lateral vertical edges of the prism. The regions where this frequency (which will be denoted as HF in the following) is particularly evident are those just outside the lateral wake boundary; the latter may adequately be detected by moving the hot-wire probe from high to low absolute values of y/w, and finding the positions corresponding to a local maximum of the kurtosis of the velocity signals. The HF peak decreases in intensity moving up in the vertical direction and increases moving downstream until $x/w \cong 2.5$, which may then be assumed to roughly correspond to the formation length of the vortices. An example of wavelet spectrum obtained in a point in which this peak dominates is shown in Fig. (2a).

As already pointed out, a lower frequency at $St \cong 0.05$ (LF in the following) was also detected in the upper part of the wake, and becomes the dominating one above $z/h \cong 1.0$ and from $x/w \cong 1.5$ to $x/w = 4.0$ (see Fig. (2b)). Both experimental and numerical analyses, [7], showed that this frequency is associated with a vertical, in-phase, oscillation of the vortical structures present in that region, i.e. both the two counter-rotating axial vortices detaching from the body free-end and the upper part of the vorticity layer that originates from the body sides and is dragged around the above-mentioned vortices.

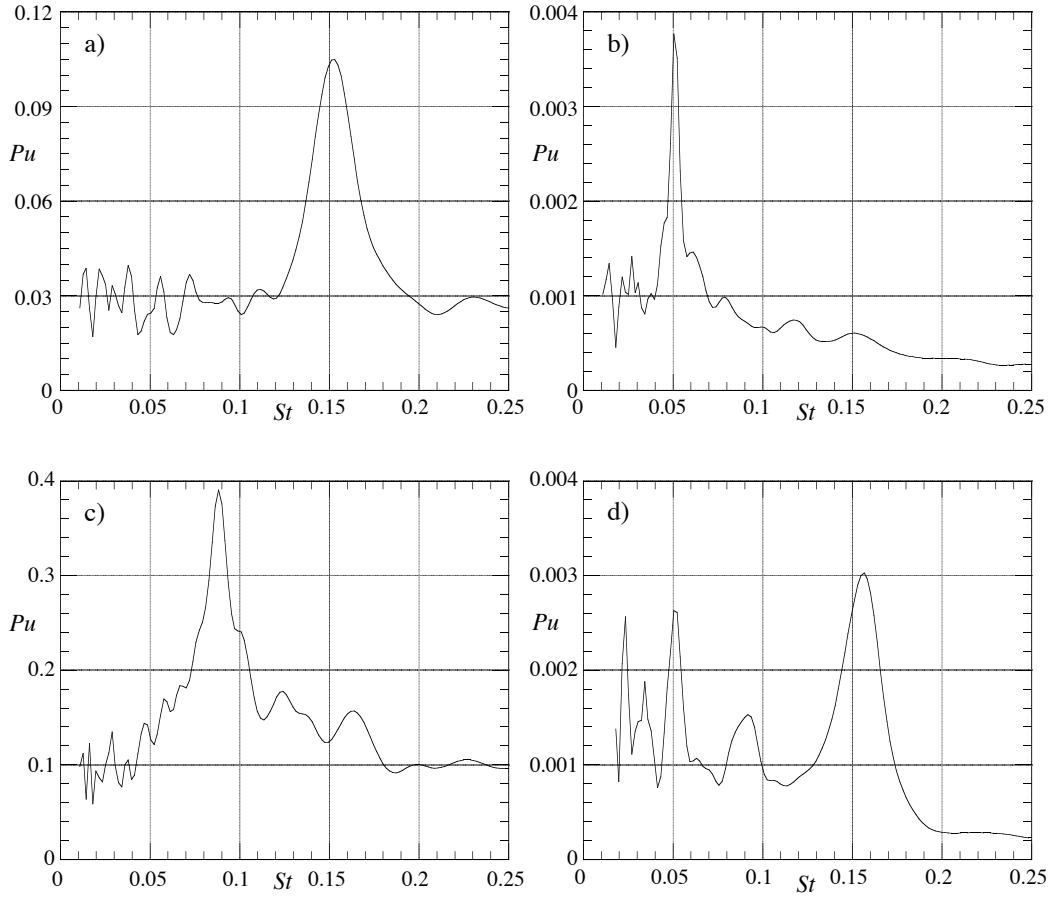

Figure 2: Examples of the wavelet spectra obtained in various regions around the wake. a) $x/w = 2.5$, $y/w = 1.0$, $z/h = 0.5$; b) $x/w = 4.0$, $y/w = 0.5$, $z/h = 1.1$; c) $x/w = 2.5$, $y/w = 0$, $z/h = 0.5$; d) $x/w = 2.5$, $y/w = 2.5$, $z/h = 0.3$.

A careful analysis of all the velocity signals showed that another spectral peak at an intermediate frequency $St \cong 0.09$ (IF in the following) becomes dominant in the wake symmetry plane $y = 0$, in positions corresponding to different stream-wise coordinates x/w depending on the vertical position; as an example, the spectrum obtained at $z/h = 0.5$ and $x/w = 2.5$ is shown in Fig. (2c). By analysing the numerical results of [7] and flow visualizations, it was suggested in [3] that the fluctuations at this frequency are caused by a flag-like oscillation of the sheet of transversal vorticity shed from the rear edge of the body free-end, and approximately lying along the downstream boundary of the recirculation region in the central part of the near wake

The three above described frequencies may also be found together in the spectra of velocity signals acquired aside the wake, sufficiently far from its boundary, Fig. (2d). In such positions the fluctuations due to vortex shedding are reduced in such a way that the peaks at the remaining frequencies become detectable. Therefore, even if the fluctuations at the various frequencies are probably produced by the dynamics of different vorticity structures, and are thus clearer near the regions where these structures are present, they all contribute to the global oscillation of the wake, which is indeed best felt further away from its boundaries.

In order to substantiate the previous physical interpretations on the origin of the IF, measurements of the mean and fluctuating pressures over significant parts of the model free-end and rear surfaces were carried out to single out the regions where the intermediate frequency dominates, and the main results of these tests are described in the following section.

3.2 Pressure measurements

Pressure measurements were first carried out over the free-end surface; a general view of the positions of the pressure taps is given in Fig. (3), where the relevant coordinates are also reported. The comparison between all the mean values of the pressure coefficients obtained in the present investigation (from at least six acquisitions for each point) and the results of the numerical simulation described in [7] is shown in Fig. (4).

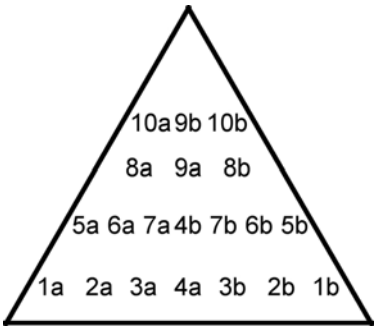

Tap #	*x/w*	*y/w*	*Tap #*	*x/w*	*y/w*
1A	–0.11	–0.37	1B	–0.11	0.37
2A	–0.11	–0.27	2B	–0.11	0.27
3A	–0.11	–0.16	3B	–0.11	0.16
4A	–0.11	0.00	4B	–0.28	0.00
5A	–0.28	–0.29	5B	–0.28	0.29
6A	–0.28	–0.21	6B	–0.28	0.21
7A	–0.28	–0.12	7B	–0.28	0.12
8A	–0.44	–0.15	8B	–0.44	0.15
9A	–0.44	0.00	9B	–0.61	0.00
10A	–0.61	–0.09	10B	–0.61	0.09

Figure 3: Positions and coordinates of pressure taps over the tip surface.

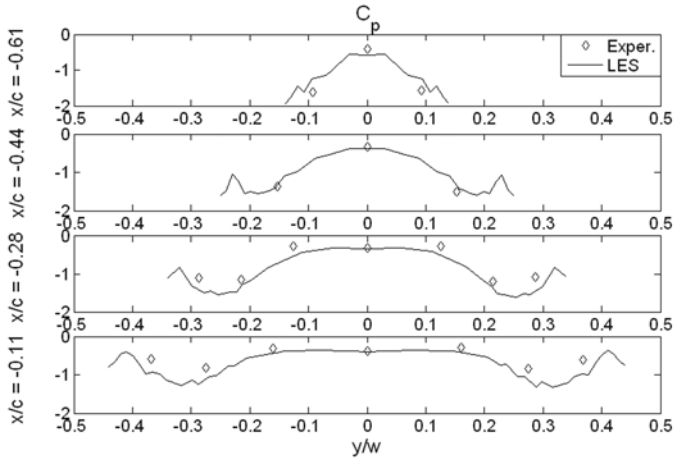

Figure 4: Comparison between experimental and numerical pressure coefficients over the tip.

As can be seen, in spite of the different values of the Reynolds number, a good agreement is found. However, in proximity to the rear edge the experimental pressure suction is slightly less intense than in the LES simulation. In other words, in the experiments the vortices seem to lift up from the tip surface slightly before than in the numerical simulation.

The analysis of the fluctuating pressure signals provides more information on the dynamics of the vorticity structures over the free-end. In Fig. (5a) the wavelet spectra of the pressure fluctuations are shown for three points along the centreline; as can be seen, the intermediate frequency (at $St \cong 0.09$) becomes dominant moving towards the rear edge of the free-end, but it is also clearly visible more upstream, together with the lower frequency (at $St \cong 0.05$) connected with the oscillation of the axial vortices. The IF is even stronger and more dominant on lateral points along the rear edge, as can be appreciated from Fig. (5b).

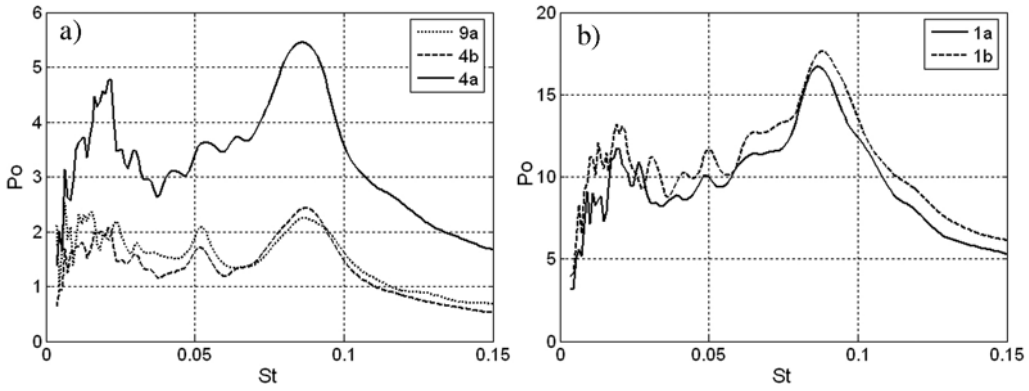

Figure 5: Wavelet spectra of pressure fluctuations at various positions over free-end surface.

The pressure measurements on the rear surface were carried out using 8 pressure taps on the symmetry plane $y/w = 0$ from $z/h = 1/9$ to $z/h = 1/2$, with a mutual vertical spacing of $\Delta z/h = 1/18$; furthermore, pressure taps were also positioned at $y/w = \pm 0.25$ and $z/h = 1/6$, 1/3 and 1/2. The results of the statistical analysis of the pressure coefficients obtained on the symmetry plane are reported in Figs. (6). In this case the measurements were carried out at two different values of *Re*, and, as can be seen, the differences are not significant.

The first point to be noticed is that a local maximum of the mean C_p is clearly present between $z/h = 5/18$ and $z/h = 6/18$ (Fig. (6a)); therefore, this region may confidently be associated with the location where, on average, the transversal shear layer impinges over the rear surface. On the other hand, the maximum value of the standard deviation is found at $z/h = 1/6$ (Fig. (6b)), showing that the pressure fluctuations are definitely higher on the portion of rear surface lying just below the recirculation region.

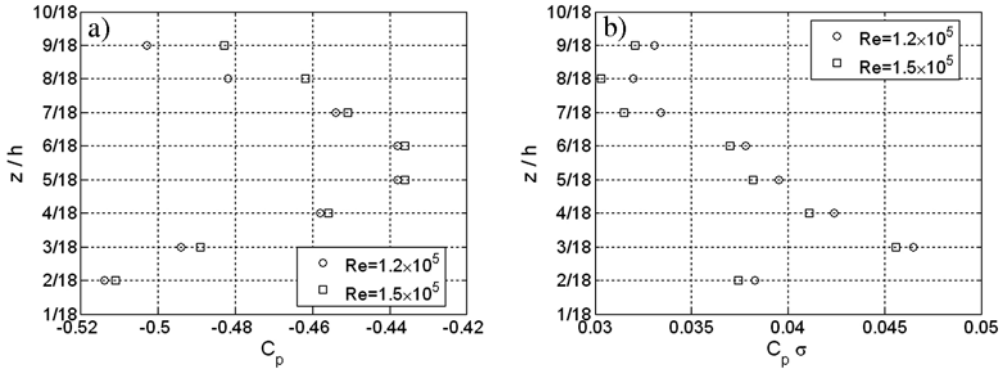

Figure 6: Pressure coefficients over rear surface at $y/w = 0$. a) mean value; b) standard deviation.

Perhaps the most interesting result, as regards the characterization and the definition of the origin of the intermediate frequency, is the variation of the spectra of the pressure fluctuations as a function of the vertical position, which is shown in Fig. (7). Indeed, the intensity of the corresponding spectral component clearly increases moving downwards, and becomes definitely dominating below the reattachment of the recirculation region. Therefore, this result, together with the dominance of this component along the rear edge of the free-end, perfectly confirm the previous interpretation on the origin of the velocity fluctuations reported in [3], and substantiate the association of the intermediate frequency with oscillations of the sheet of transversal vorticity bounding the recirculation region behind the body.

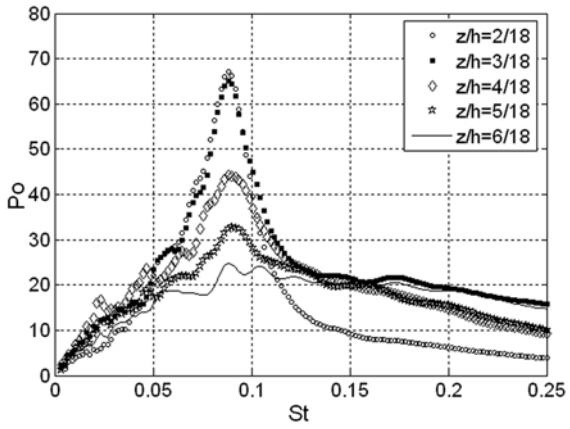

Figure 7: Wavelet spectra of pressure fluctuations over rear surface at $y/w = 0$. $Re = 1.5 \cdot 10^5$.

Finally, to further characterize the fluctuating pressure field over the rear surface, the correlation between couples of pressure signals acquired in different positions was evaluated. To this end, the method described in [6] was used, which consists in extracting the spectral components of interest from the two signals and calculating their cross-correlation through the *Hilbert Local Correlation Coefficient*, *HLCC*. The latter provides the time variation of the cross-correlation coefficient between two signals having similar frequencies.

The procedure was applied to pairs of signals acquired either in different positions along the centreline, or in symmetrical positions on its sides (i.e. $y/w = \pm 0.25$). In all cases the median value of *HLCC* was found to be around 0.94, which suggests that the oscillations of the whole shear layer bounding the recirculation region are in phase and have a global effect, causing almost simultaneous pressure fluctuations over the rear surface.

More details on the analysis of all the obtained pressure signals may be found in [8].

4 RESULTS FOR THE MODIFIED MODELS

4.1 Modifications of the vertical edges of the prism

Having confidently established the relation between the dominating frequencies found in the wake of the prism and the dynamics of different vorticity structures, it was decided to deeper investigate on the possible connection between the various frequencies. To this end, geometrical modifications were introduced on the model in order to successively interfere with the dynamics of the single vorticity structures.

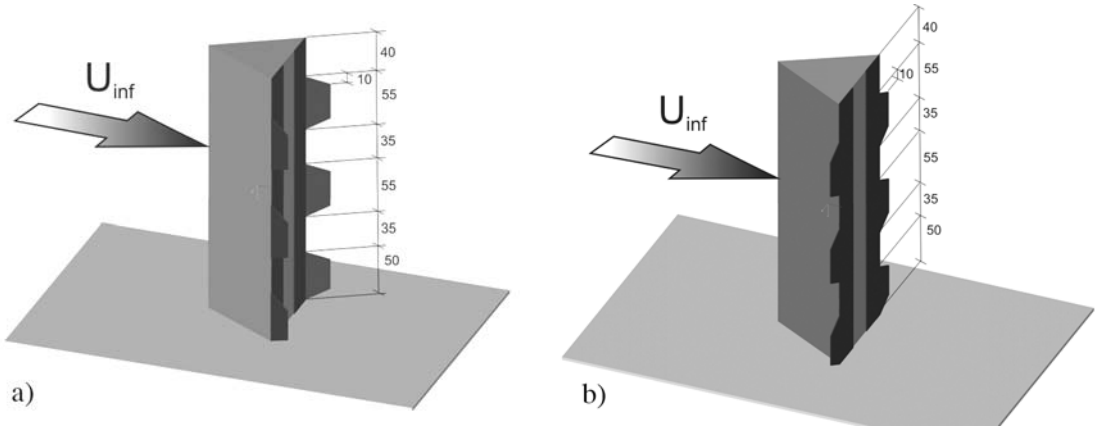

Figure 8: Geometrical modifications to affect the alternate vortex shedding: a) Mod1; b) Mod2.

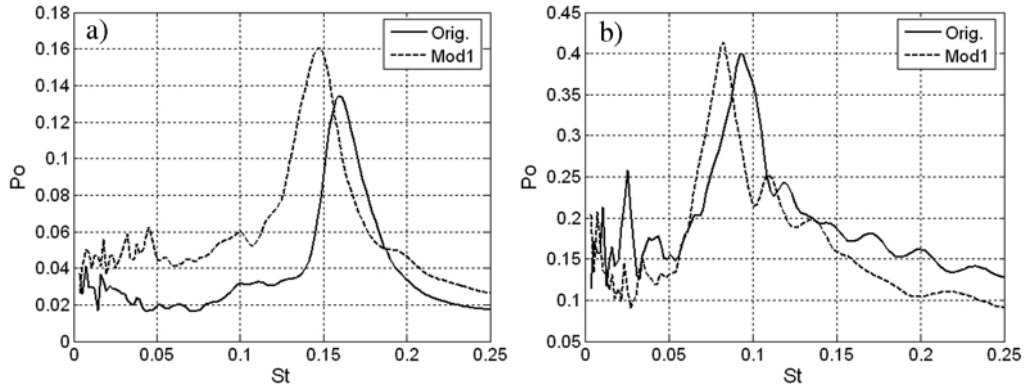

Figure 9: Wavelet spectra for original and Mod1 configurations.
a) $x/w = 4$, $y/w = -1.5$, $z/w = 0.3$; b) $x/w = 2.75$, $y/w = 0$, $z/w = 0.4$.

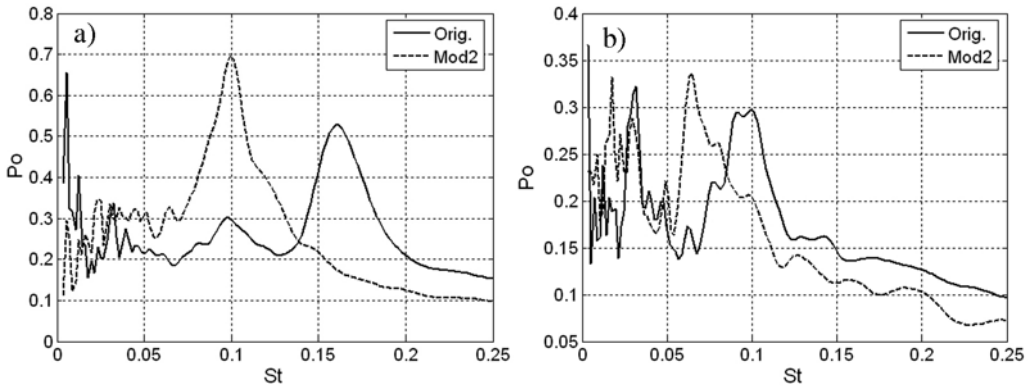

Figure 10: Wavelet spectra for original and Mod2 configurations.
a) $x/w = 2.5$, $y/w = -0.88$ (orig.), $y/w = -1.5$ (Mod2), $z/w = 0.3$; b) $x/w = 2.875$, $y/w = 0$, $z/w = 0.3$.

The first attempt was to alter, and possibly inhibit, the vortex shedding mechanism by introducing three-dimensional modifications to the lateral edges of the model. In particular, 20 mm high trapezoidal indentations were placed extending either the lateral surfaces or the rear surface (respectively Mod1 and Mod2 in Fig. (8)).

In Figs. (9) and (10) the spectra of hot-wire signals from positions where the vortex shedding or the intermediate frequencies were dominant are reported for the original and modified models. As can be seen (Figs. (9a) and (10a)), with neither modification the frequency associated with vortex shedding disappears, even if a lowering of its value is found, which, as will be seen, is in strict connection with the increase of the mean wake width.

Particularly interesting is the Mod2 case, for which, in spite of the significant geometrical disturbances introduced along the lateral edges, the vortex shedding is apparently still present, and the large widening of the wake produces much stronger fluctuations, which are felt even close to the free-end and at larger lateral distances. This is why in Fig. (10a) the comparison is made for different lateral positions for the original and modified models, to allow the same scale to be used.

To further characterize the wake variations introduced by the modifications to the lateral vertical edges of the prism, hot-wire wake surveys were carried out, which are described in detail in [8]. Here only the standard deviations obtained at two different downstream sections of the wake and various vertical coordinates are shown in Fig. (11) for the original model and the Mod2 configuration. The significant increase of the width of the wake for the modified model is evident; furthermore, the increased fluctuations for $x/w = 4$ and $z/h = 1.1$ suggest that the vertical size of the wake is also increased.

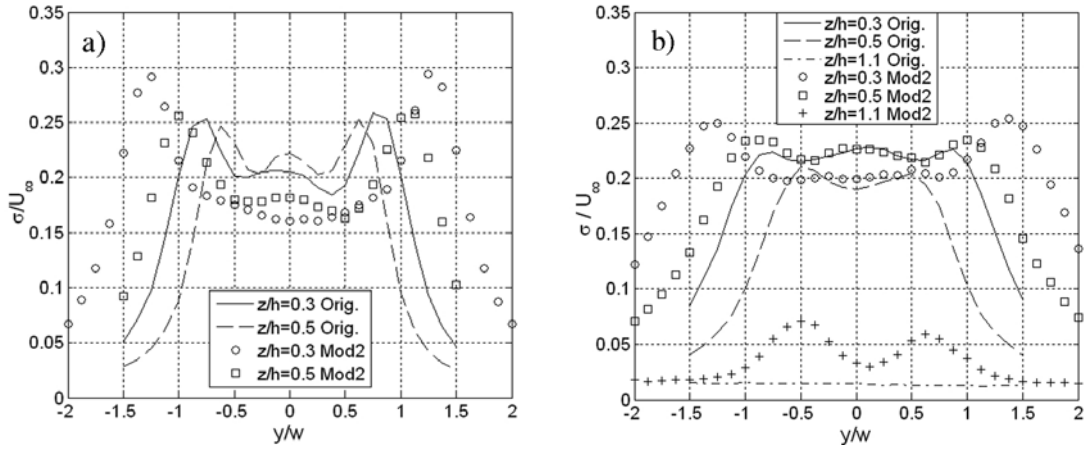

Figure 11: Standard deviations of the h-w signals for the original model and Mod2. a) $x/w = 2.5$, b) $x/w = 4$.

The Strouhal number of the HF, which was $St \cong 0.16$ for the original model, was found to change to $St \cong 0.142$ for Mod1 and $St \cong 0.098$ for Mod2, in an almost perfect inverse relation to the increase of the wake width.

For the original and Mod2 models, simultaneous measurements of the velocity fluctuations on the two sides of the wake boundary were carried out by using two hot-wire probes. The analysis of the signals through the wavelet-Hilbert technique confirmed that also for Mod2 the HF frequency is indeed related to an alternate vortex shedding, even if, as could have been expected, with a different level of regularity. In effect, the median values of *HLCC*, obtained using comparable procedures, were $HLCC \cong -0.94$ with a standard deviation of $\cong 0.18$ for the original model, and $HLCC \cong -0.84$ with a standard deviation of $\cong 0.45$ for Mod2.

Considering now the connection between the various frequencies, an important point arising from Figs. (9b) and (10b) is that the intermediate frequency decreases roughly in proportion to the vortex shedding frequency. This result may be explained by considering that, according to the previously described physical interpretation, this frequency is connected with the oscillations of the recirculation region; now, the widening of the wake for the modified models is likely to produce a similar variation of the length of the recirculation region, which is the reference length for the intermediate frequency. Anyway, particularly for the Mod2 case, the unsteadiness and modulations of this component were also found to be higher.

On the other hand, as will be better described in the following section, the modifications to the lateral edges of the prism did not produce any significant variation in the LF fluctuations in the upper wake region.

Finally, the drag forces acting on the three models were measured through the strain-gage balance. To allow a sensible comparison to be carried out, the corresponding drag coefficients were evaluated using the effective area of the cross-flow projection of the three models as reference surface, and the obtained results are reported in Table 1. As can be seen, the values of the drag coefficient are the same for the original and the Mod1 models. Conversely, a significantly higher value was found for the Mod2 configuration; this result is certainly due to the considerably wider wake of this model, caused by the orientation of the introduced indentations, and to the intense vortex shedding that was still found to characterize its wake.

Original	Mod1	Mod2
0.82	0.82	1.18

Table 1: Drag coefficients based on the cross-flow area for original and modified models.

4.2 Modifications of the free-end edges of the prism

To try to interfere with the dynamics of the vorticity structures originating from the free-end, geometrical modifications to its edges were introduced. In particular, to directly influence the structure of the shear layer bounding the recirculation zone, and, consequently, the intermediate frequency, the rear free-end edge was first modified, by adding to it triangular indentations (Mod3, Fig (12a)) and an elongation with a circular arc plate (Mod4, Fig (12b)).

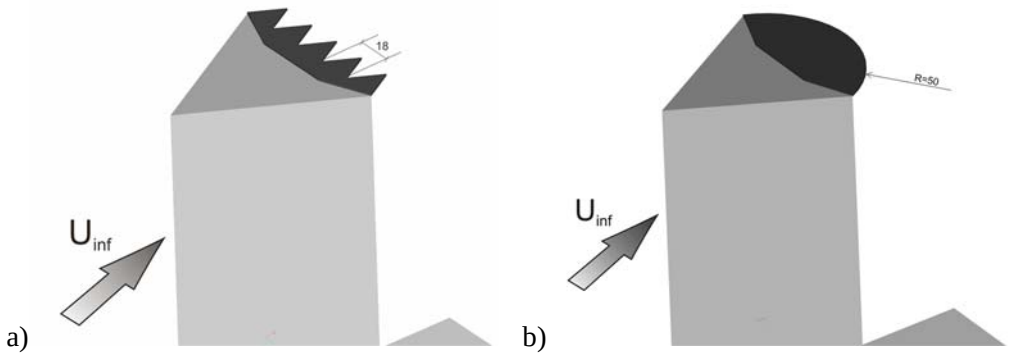

a) b)

Figure 12: Geometrical modifications to affect the intermediate frequency: a) Mod3; b) Mod4.

The results of the survey of the wake velocity fluctuations showed that the effects of these modifications on the wake morphology were definitely negligible. In particular, the spectra showing the dominating peak at the vortex shedding frequency (not reported here for sake of brevity) remained practically unaltered; this could be expected, as no interference with the shear layers detaching from the lateral vertical edges was introduced. But even the intermediate frequency, which might have been presumed to be affected, showed virtually no change both in frequency and energy, as can be appreciated from Fig. (13).

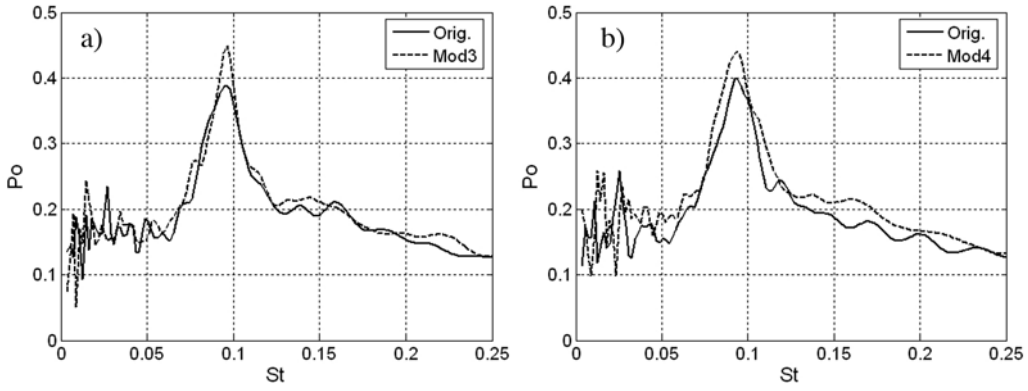

Figure 13: Wavelet spectra for original and modified configurations.
a) Mod3, $x/w = 3$, $y/w = 0$, $z/w = 0.4$; b) Mod4, $x/w = 2.875$, $y/w = 0$, $z/w = 0.4$.

As for the lower frequency at $St \cong 0.05$, which had been found to dominate in the upper part of the wake, all the above described modifications did not produce any noticeable variation, thus demonstrating that it is not connected with the vortex shedding frequency or with the width of the wake. This is clearly seen from Fig. (14), where the spectra for the original and modified models, obtained at high lateral positions, are compared. Incidentally, Fig. (14a) also shows that the fluctuations at the vortex shedding frequency for the Mod2 configuration have a much higher intensity; in effect, for this case the associated peak is clearly detectable even in this position, together with a small peak also at the intermediate frequency.

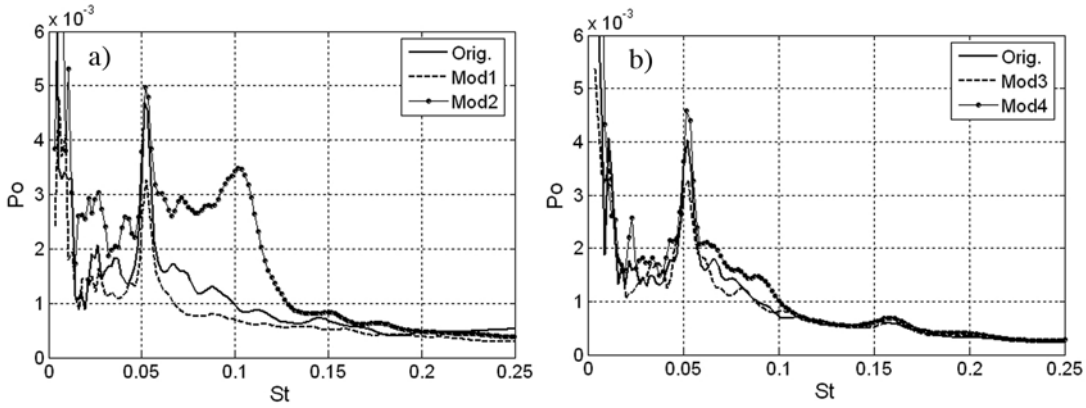

Figure 14: Wavelet spectra for original and modified configurations.
a) Mod1 and Mod2, $x/w = 4$, $y/w = -1.5$, $z/w = 1.1$; b) Mod3 and Mod4, $x/w = 4$, $y/w = -1.5$, $z/w = 1.1$.

In an attempt of directly interfering with the physical mechanism originating the low frequency, the front edges of the free-end were then modified in order to influence the roll-up of the shear layers and the formation of the free-end axial vortices. In particular, 10 mm high rectangular plates were added, both parallel and orthogonal to the upper surface (Mod5, Fig. (15a)). However, rather surprisingly, once again no variation was found in the frequency, energy and regularity of the fluctuations in the upper part of the wake, as may clearly be seen from the spectra of Fig. (15b). This suggests that, in spite of the highly irregular free-end edge, the mechanism of roll-up of the vorticity shed from the lateral sides is still strong enough to be able to generate the axial counter-rotating vortices whose dynamics was considered to be responsible for the presence of the low frequency.

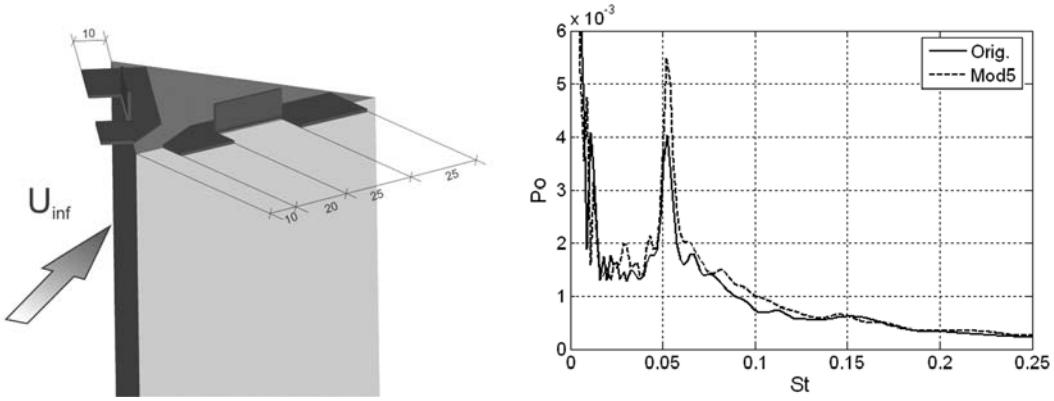

a) b)

Figure 15: Modification of free-end front edges: a) Mod5; b) spectra at $x/w = 4$, $y/w = -1.5$, $z/w = 1.1$.

In order to confirm the above conjecture, and also to characterize possible differences in the formation processes of the axial vortices for the two cases, flow visualizations were used to compare the near upper wake geometries of the original model and of the Mod5 configuration.

The images obtained for the original model by setting the laser sheet in two different vertical planes orthogonal to the free-stream direction, with the camera directed upstream, are shown in Fig. (16), with inverted gray levels.

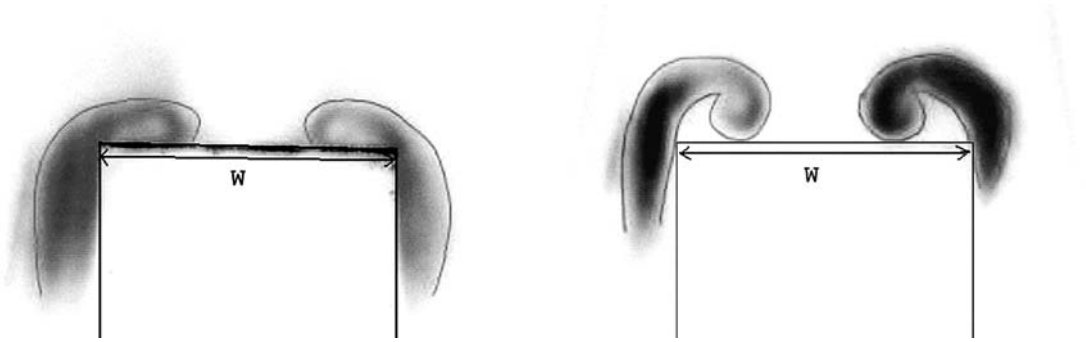

a) b)

Figure 16: Flow visualizations in vertical cross-flow planes over original model free-end. Inverted gray levels. a) $x/w = 0$; b) $x/w = 0.25$.

The visualizations largely confirmed the complex upper wake flow structure highlighted from the numerical simulations in [7]. In particular, the shear layers from the upstream surfaces, which are visualized by the smoke, are seen to wrap around the two counter-rotating vortices detaching from the front inclined edges of the free-end, whose lateral position is about $y/w = \pm 0.3$, in good agreement with the LES results and previous experimental findings described in [1].

Fig. (17) shows the visualizations obtained for the Mod5 model for the same vertical planes reported in Fig. (16), and for two planes placed more upstream. The main point that can be deduced from the comparison between the two cases is that the axial vortices are still generated downstream of the modified model, but with a completely different formation process. In particular, smaller vortices are produced along the edges of the plates that were added on each side of the free-end. However, these vortices, which have the same sign, coalesce in a single vortex behind the free-end, so that, eventually, a couple of counter-rotating vortices is produced which is comparable to the one deriving from the original model.

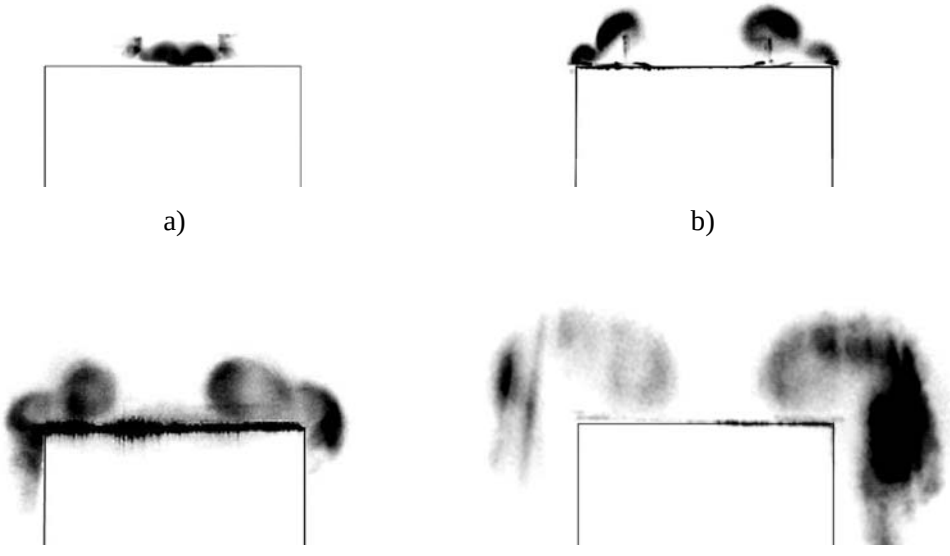

a) b)

c) d)

Figure 17: Flow visualizations in vertical cross-flow planes over Mod5 free-end. Inverted gray levels. a) $x/w = -0.67$; b) $x/w = -0.17$; c) $x/w = 0$; d) $x/w = 0.25$.

Just as interesting are the visualizations obtained by positioning the laser sheet in longitudinal vertical planes, and in particular in the symmetry plane and in a plane passing through the position of the axial vortices, which are shown in Fig. (18) for the two models.

First of all, for the original model (Figs. (18a) and (18b)) a confirmation is obtained of the different height of the wake boundary in the two planes; moreover, the transversal shear layer detaching from the rear edge of the free-end is seen to rapidly bend downwards inside the wake, forming the boundary of a recirculation region behind the body, similarly to what was found in the LES simulation of [7]. Consequently, this shear layer apparently impinges on the rear model surface at a low vertical coordinate, confirming the previously-described findings from the pressure measurements.

As for the modified model (Figs. (18c) and (18d)), the visualizations show that the height of the wake boundary is definitely similar to that of the original model, thus confirming a comparable strength of the axial vortices released in the wake in the two cases. This may explain why no variation of the LF was found from the hot-wire measurements.

Finally, it must be pointed out that the images of the visualizations described herein are derived from digital videos which, in all the analysed cases, showed a significant unsteadiness of the flow, with the presence of oscillations of the whole recirculation region at very low frequencies.

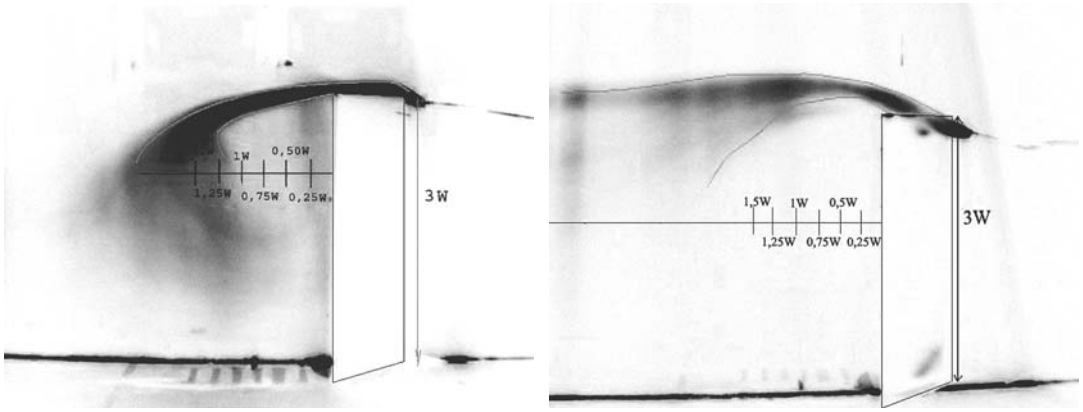

a) b)

c) d)

Figure 18: Flow visualizations in vertical longitudinal planes. Inverted gray levels.
a) Original model, $y/w = 0$; b) Original model, $y/w = 0.3$; c) Mod5, $y/w = 0$; d) Mod5, $y/w = 0.35$.

5 DISCUSSION AND CONCLUSIONS

The first purpose of this work was to gather further experimental evidence to substantiate previous physical interpretations on the connection between the observed fluctuations and the dynamics of different vorticity structures in the wake of a prism with equilateral triangular cross-section, placed vertically on a plane with its apex edge against the incoming flow.

Flow visualizations using smoke and a laser sheet confirmed the complex topology of the upper part of the near wake previously deduced from a LES numerical simulation; in particular, the shear layers from the upstream surfaces are seen to wrap around two counter-rotating vortices detaching from the front inclined edges of the free-end, and to produce a significant difference between the vertical position of the middle and lateral parts of the upper boundary of the wake. Furthermore, in the central portion of the near wake a recirculation region is present, and is bounded by the shear layer formed by the transversal vorticity shed from the rear edge of the free-end, which impinges on the lower part of the rear model surface.

The presence, intensity and regions of prevalence of three different frequencies in the wake fluctuations were then characterized by means of careful hot-wire surveys. In particular, the frequency connected with alternate vortex shedding from the lateral vertical edges of the prism, with a Strouhal number $St = fw/U \cong 0.16$, was found to dominate in the zones outside the lateral boundary of the wake, for vertical positions below $z/h = 0.9$. A lower frequency, at $St \cong 0.05$, was found to prevail in the velocity fluctuations in the whole upper wake, for downstream distances $x/w \geq 1.5$; this frequency is associated with a vertical, in-phase, oscillation of the vorticity structures detaching from the free-end. Fluctuations were also observed at an intermediate frequency $St \cong 0.09$, and to be dominant in positions corresponding to the downstream boundary of the recirculation region in the central part of the near wake.

Measurements of the mean and fluctuating pressures over the tip and rear surfaces of the model completely confirmed the suggestion that the origin of the intermediate frequency may be an oscillation of the transversal vorticity sheet bounding the recirculation region behind the body. Peaks at this frequency were indeed found to dominate in the spectra of the pressure signals acquired both near the rear edge of the free-end and below the reattachment point on the rear surface, over which the corresponding fluctuations were also found to be in phase.

Subsequently, geometrical modifications of the model were carried out in order to vary the evolution and dynamics of the vorticity structures originating from the edges of the prism, and to characterize the possible connection between the various frequencies.

With the objective of altering, and possibly inhibiting, the vortex shedding mechanism, trapezoidal indentations were first added to the lateral edges of the model, extending either its lateral surfaces or its rear surface. The rationale behind these modifications was that the introduction of a considerable non-uniformity, both in model width and flow direction, along the height of the model might hinder the production of a regular vortex shedding with constant frequency. Conversely, and somewhat surprisingly, the hot-wire analysis of the wake flow fluctuations showed that strong alternate vortex shedding was still present in the modified configurations (even if with a slightly reduced regularity), and that the relevant Strouhal number decreased in close connection with the increase in the mean wake width. This finding is a further confirmation of the strength of the instability mechanism leading to alternate vortex shedding, and suggests that its domain of existence is definitely larger than could be expected.

As for the intermediate frequency, it was found to closely follow the variation of the vortex shedding frequency; this substantiates its connection with the length of the recirculation boundary, which is likely to be proportional to the width of the wake. On the other hand, no variation of this frequency was found when the rear edge of the free-end was modified by means of indentations or of an elongation with a circular arc plate. This result may be due to

the fact that these modifications did no actually vary the amount of the transversal vorticity component being introduced in the wake, which is thus confirmed to be the important feature driving the oscillations at the intermediate frequency.

All the above geometrical modifications were found not to alter the lower frequency fluctuations in the upper part of the wake, connected with the oscillation of the axial vortices detaching from the lateral edges of the body free-end. Actually, this frequency remained unaltered even when these edges were made irregular by means of rectangular plates with alternately parallel and orthogonal orientation relative to the model upper surface. In effect, flow visualizations showed that the near wake of the modified model is similar to that of the original prism, and that axial vortices are still generated from the free-end, even if with an entirely different formation process. In particular, smaller vortices of the same sign are produced along the edges of the plates on each side of the free-end, and then rapidly coalesce in a single vortex; consequently, the two counter-rotating vortices that are eventually produced are comparable to those deriving from the original model, even if perhaps slightly more diffuse.

ACKNOWLEDGEMENTS

The financial support of the Italian Ministry of University and Research, M.U.R., is gratefully acknowledged.

REFERENCES

[1] G. Buresti, G. Lombardi. Experimental analysis of the free-end and upper wake flow fields of finite triangular prisms. Atti del 7° Convegno Nazionale di Ingegneria del Vento, In-Vento-2002 (Diana G., Cheli F., Zasso A., Eds.), 375-382. SGEditoriali, 2002.

[2] G. Buresti, G. Lombardi. Experimental analysis of the upper-wake flow field of finite cylinders with triangular and circular cross-section, Atti XVI Congresso AIMETA, Ferrara, CD Rom, 2003.

[3] G. Buresti, G.V. Iungo. Characterization of the velocity fluctuations in the wake of a triangular prism of moderate aspect-ratio. Atti XVII Convegno Nazionale AIMETA, Firenze University Press, CD Rom, 2005.

[4] T. Kitagawa, T. Wakahara, Y. Fujino, K. Kimura. An experimental study on vortex-induced vibration of a circular cylinder tower at a high wind speed. *Journal of Wind Engineering and Industrial Aerodynamics*, **69-71**, 731-744, 1997.

[5] C.-W. Park, S.-J. Lee. Free end effects on the near wake flow structure behind a finite circular cylinder. *Journal of Wind Engineering and Industrial Aerodynamics*, **88**, 231-246, 2000.

[6] G. Buresti, G. Lombardi, J. Bellazzini. On the analysis of fluctuating velocity signals through methods based on the wavelet and Hilbert transforms. *Chaos, Solitons & Fractals*, **20**, 149-158, 2004.

[7] S. Camarri, M.V. Salvetti, G. Buresti. Large-eddy simulation of the flow around a triangular prism with moderate aspect-ratio. *Journal of Wind Engineering and Industrial Aerodynamics*, **94**, 309-322, 2006.

[8] G.V. Iungo, G. Buresti - Experimental investigation on the wake generated from a low aspect-ratio triangular prism in cross-flow. *Atti del Dipartimento di Ingegneria Aerospaziale*, N° ADIA 2007-4, ETS Editrice, Pisa, June 2007.